ELECTRICAL PROPERTIES OF THE HETEROJUNCTION IN $Cu(In,Ga)Se_2$ SUPERSTRATE SOLAR CELLS

F.-J. Haug*, D. Rudmann, A. Romeo, H. Zogg, A. N. Tiwari♯, Swiss Federal Institute of Technology (ETH) Zürich, Thin Film Physics Group, Technoparkstrasse 1, CH-8005 Zürich, Switzerland
* Swiss Federal Laboratories for Material Testing and Research (EMPA), Überlandstrasse 129, CH-8600 Dübendorf
♯Also: Department of Electronic and Electrical Engineering, Loughborough University, Leicestershire, LE11 3TU, United Kingdom

ABSTRACT

The electrical properties of heterojunctions between wide gap n-type oxides and the p-type semiconductor $Cu(In,Ga)Se_2$ have been studied. The investigated oxides were a bilayer of undoped and aluminium doped ZnO, and the commercially available transparent conducting oxides SnO_2:F (FTO) and In_2O_3-SnO_2 (ITO). The junction of CIGS with ZnO showed the characteristic of a pn-junction, the temperature dependence of the current-voltage characteristics suggests interface recombination as dominating transport mechanism. This junction is suitable for photovoltaic light conversion and for the development of solar cells in superstrate configuration. The junctions of CIGS with FTO and with ITO showed poor rectifying behaviour and little or no response to illumination. The quasi-ohmic behaviour of these junctions was successfully used to replace the Molybdenum back contact with a transparent back contact in $Cu(In,Ga)Se_2$ substrate solar cells.

1. INTRODUCTION

Solar cells with $Cu(In,Ga)Se_2$ (CIGS) absorber layers have proven their suitability for high efficiency and stable low cost solar cells. They are generally grown on glass coated with a molybdenum back contact. In this substrate configuration their light conversion efficiencies approach 19% [1, 2]. In an alternate configuration the deposition process is started with the transparent conducting oxide rather than with the metal. This so called superstrate configuration is advantageous because it allows illumination through the supporting glass. Thus, superstrate solar cells promise lower manufacturing costs due to easier encapsulation, and they are also important for the development of advanced tandem solar cells where they will be used as absorber for the short wavelength part of the solar spectrum. The efficiencies of CIGS superstrate solar cells are in the range of 11 to 13% [3, 4].
Recently, the junctions between CIGS and n-type FTO and ITO have gained attention because they do not exhibit the behaviour of pn-junctions, rather, ohmic or quasi-ohmic characteristics are observed. These transparent conducting oxides (TCOs) have been successfully used to replace the metallic back contact in substrate type cells, resulting in semi-transparent solar cells [5, 6, 7].
We have prepared heterojunctions between CIGS and ZnO/ZnO:Al as well as directly to the transparent conductors FTO and ITO, and studied the electrical properties of these junctions with measurements of the temperature dependence of their current-voltage characteristics.

2. BAND ALIGNMENT

The alignment between the conduction bands in the p- and n-side of the junction is important for the performance of solar cells because it has a strong influence on the current transport across the heterojunction. The properties of the conduction bands are usually determined indirectly by measuring the positions of the valence bands with photoelectron spectroscopy and adding the values of the band gaps [8]. If a discontinuity is detected, two cases are distinguished, the cliff- and the spike-type. Modeling of the heterojunction in CIGS solar cells showed that a conduction band alignment of the cliff-type is generally detrimental to the device, whereas a spike of up to 0.3 eV does not harm the performance [9] or is even considered favourable for minimizing recombination loss under operating conditions [10, 11, 12].

2.1 The junction between ZnO and CIGS

The valence band offset between CIGS and undoped ZnO ranges from 2.3 to 2.4 eV [13, 14]. The band gap of undoped ZnO is 3.3 eV, in CIGS it depends on the composition. For a Ga/(Ga+In) ratio of 0.25 which is frequently employed in solar cells the band gap is approximately 1.2 eV. The energy band diagram of the heterojunction between ZnO and CIGS is shown in figure 1. In case of undoped ZnO the conduction band shows a discontinuity of the cliff-type with a magnitude of approximately -0.3 eV.
The resulting band bending in equilibrium depends on the Fermi-level positions in the ZnO and the CIGS. For ZnO a value of 0.1 eV below the conduction band minimum (CBM) is assumed, this corresponds to a carrier concentration just below the limit to degener-

acy and may serve as upper limit. In the investigated CIGS layers carrier densities of about 10^{15} cm^{-3} are measured after light soaking [15], corresponding to a Fermi level about 0.2 eV above the valence band maximum (VBM). Thus, under open circuit conditions a band bending qV_{bi} of 0.6 eV is estimated. Due to the high carrier density in ZnO the band bending is expected to occur mostly in the absorber layer.

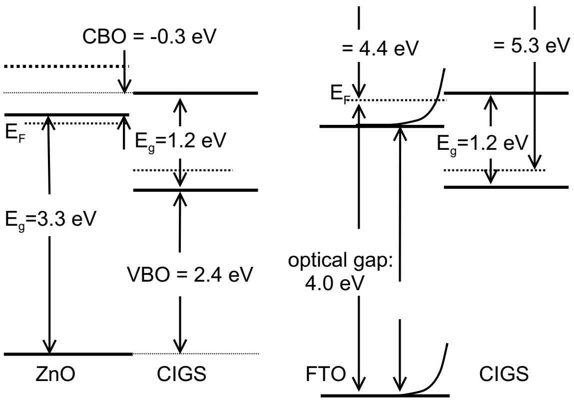

Fig. 1: Band alignment between CIGS and ZnO (left) and FTO (right). In the first case the conduction band offset is of the cliff type and amounts to approximately -0.3 eV. The dotted line illustrates a spike type alignment e.g. with a (Zn,Mg)O buffer layer [11]. To the right the alignment of CIGS/FTO is shown, the conduction band offset depends on the particular properties of the TCO.

2.2 Junctions between CIGS and FTO and ITO

Little data exists about the band alignment between CIGS and SnO_2. An idea can still be obtained by combining data on the band alignment between CdS and SnO_2 [16] and between CdS and CIGS [13, 17]. This yields values for the valence band offset in the range from of 2.2 to 2.5 eV.

The band gap in SnO_2 varies between 3.6 eV (undoped [16]) and 4.5 eV (optical gap in degenerately doped SnO_2:F (FTO) [18]). The differences in these values are related to the high carrier concentration which is accomodated by a partial filling of the conduction band (Burstein-Moss shift) [19]. At the same time merging of donor states with the band edge may occur, resulting in a reduced gap between valence band maximum and conduction band minimum [20]. Transmission measurements of the FTO layers used here revealed an optical gap of about 4.0 eV. With an assumed carrier density of 10^{21} cm^{-1} and an effective mass of 0.45 [18] the Fermi level is estimated about 0.4 eV above the CBM, indicating that no band gap narrowing is present in FTO. The range for the conduction band offset is then estimated between -0.1 (cliff) and +0.2 eV (spike) with built-in voltages between 1.3 and 1.5 eV.

A different situation is obtained from a consideration of the work functions. For CIGS the reported values range between 5.3 and 5.4 eV (values for ternary CIS [17, 21] and CGS [22]). Some uncertainty is involved in the work function of FTO, values of 4.4 (FTO [23]) and 4.8 (SnO_2 [24]) are reported. By combining these values the band bending would assume lower values between 0.5 and 0.9 eV. Figure 1 illustrates the band properties for an assumed FTO work function of 4.4 eV and a conduction band filling of 0.4 eV due to degeneracy.

For the determination of the conduction band alignment further complications arise from the existence of a surface depletion layer which has been reported for FTO [25]. This leads to a band bending in the surface region and a Fermi level position which is pinned 0.5 eV below the CBM. The surface depletion region in FTO has been reported to remain during later CdS deposition, but it is not known how it will be affected by CIGS deposition. The two limiting arrangements of the conduction band alignment with and without surface depletion layer in FTO are illustrated in figure 1.

A considerable amount of uncertainty is involved in estimating the band alignment between CIGS and ITO because different In_2O_3-SnO_2 mixtures are used and also because the work function of ITO depends on the sample treatment [23]. Work functions between 4.4 and 4.8 eV have been published [23, 26] and also for ITO a surface depletion layer with a Fermi level about 1.0 eV below the CBM has been reported [26].

3. EXPERIMENTAL

Heterojunctions between CIGS and different wide gap n-type materials were prepared by vacuum evaporation of Cu, In, Ga, and Se in order to grow approximately 2 µm thick layers of CIGS. The evaporation fluxes were controlled in order to yield a three step deposition process: In the first step only In, Ga, and Se are evaporated, then Cu is added in order to obtain a Cu-rich growth regime, finally in the third step the Cu flux is stopped and the endpoint detection technique [27] is used to adjust for the desired Cu-poor composition of the absorber layer. The Ga/(In+Ga) ratio is approximately 0.25. The back ohmic contact to CIGS was prepared by evaporating a 50 nm thick gold layer through an aperture mask with circular openings of 0.125 cm^2. This results in 12 to 16 individual solar cells on two 30 × 30 mm^2 substrates per deposition run.

Soda lime glass coated with ZnO/ZnO:Al bilayers, FTO, and ITO, respectively, was used as substrate material. The deposition of the ZnO:Al layers by rf magnetron sputtering on glass has been described elsewhere [28], while commercially available FTO and ITO coated glass substrates were used.

4. RESULTS AND DISCUSSION

4.1 Current voltage characteristics

The room temperature current voltage characteristics of the three different junctions are compared in figure 2. The CIGS/ZnO and CIGS/FTO junctions show a large difference in their saturation currents. On CIGS/FTO and particularly on CIGS/ITO very poor rectifying behaviour is observed. However, the purely Ohmic behaviour which has been reported for these junctions [6] was not obtained. Nevertheless, there is a considerable conduction down to about -50 mV reverse bias in CIGS/ITO, the resistance area product in the linear part around the origin is approximately 6 Ωcm^2.

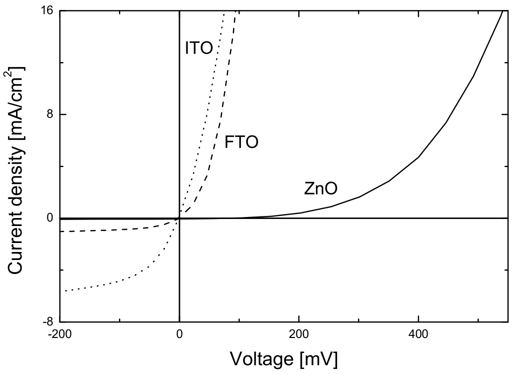

Fig. 2: Comparison of dark $j-V$ characteristics of the different types of junction. The characteristic of the CIGS/ITO junction shows poor rectifying behaviour. High leakage currents are observed down to bias voltages of -50 mV. Around the origin the characteristic resembles ohmic rather than diode behaviour.

4.2 Temperature dependence

The dark $j-V$ characteristics of the junctions were measured in the temperature range between 290 and 350 K after a stabilizing light soaking treatment. The characteristics were fitted to a one diode model with dark saturation current density j_0 and diode quality factor A.

$$j = j_0 \left(\exp\left\{ \frac{q(V - jR_s)}{AkT} \right\} - 1 \right) + \frac{V - jR_s}{R_p} \quad (1)$$

Here k is the Boltzmann constant, q the elementary charge, T is the absolute temperature, R_s and R_p denote series and parallel resistance area products, respectively.
Figure 3 presents the dependence of the dark saturation current densities and the diode quality factors on the device temperature for the junctions of CIGS to ZnO and FTO. In both cases the Arrhenius plot of the saturation current density j_0 shows a linear dependence with an activation energy E_A:

$$j_0 = j_{00} \exp\left\{ -\frac{E_A}{kT} \right\} \quad (2)$$

Here, j_{00} denotes the saturation current density prefactor. The activation energy of the junction to ZnO is 0.5 eV, while it is 0.3 eV on CIGS/FTO. The right-hand part of figure 3 shows the values of the diode quality factors in a convenient reciprocal representation [29]. The diode quality factors of the investigated junction are around 1.5 (CIGS/ZnO) and 1.2 (CIGS/FTO), and they show only little changes in the investigated range of temperatures.

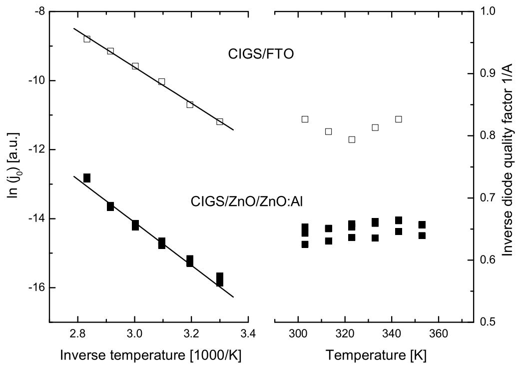

Fig. 3: Dark diode parameters for three different CIGS/ZnO junctions (full symbols) and the junction between CIGS and FTO (open symbols).

The product of the diode quality factor A and the activation energy E_A should correspond to the band gap energy if the current transport is dominated by diffusion or recombination in the space charge region [30]. The lower values of the shown examples are an indication for interface recombination. However, in this case the diode quality factor should be one or asymptotically approach unity at high temperatures in cases where the transport is assisted by tunneling [29]. In fact, in figure 3 the small variations of $1/A$ in the junction of CIGS/ZnO might be interpreted as tail of an asymptotic approach into a limiting value. Unfortunately, due to the limited temperature range of this investigation a clearer identification is not possible. However, it is clear that the values do approach a value around 1.5 rather than unity. This behaviour would require that the band bending extends also into the n-type part of the junction, similar to observations in early $CdS/CuInSe_2$ solar cells [10, 31, 32]. In this case, the following relation for the saturation current would apply:

$$j_0 = qSN_V \exp\left\{ -\frac{qV_{D,p} + \delta_p}{kT} \right\} \quad (3)$$

Here S denotes the interface recombination velocity and N_V is the effective density of states in the p-layer. The activation energy E_A is then given by the sum of $qV_{D,p}$, the band bending in the p-part of the junction, and δ_p, the separation between Fermi-level and valence band maximum. The total band bending or built-in voltage V_{bi} is then given by [31]:

$$V_{bi} = A \cdot V_{D,p} \quad (4)$$

The values for the junction to ZnO yield $qV_{D,p} =$ 0.5 eV - 0.2 eV = 0.3 eV. Multiplied with the average diode quality factor an overall band bending somewhat below 0.5 eV is obtained. Considering the uncertainties in the valence band offset and the band gaps, this is in reasonable agreement to the value of 0.6 eV which was proposed in the band diagram in figure 1.

However, it is not clear, why a considerable part of the band bending should occur in the n-layer. Even without intentional doping the carrier density in ZnO should be much higher than in the CIGS layer. A possible explanation might be a potential drop in the interfacial oxide layer which has been found in the C(I)GS/ZnO junction [33, 34]. The presence of such oxide layers in Schottky junctions has been reported to lower the measured activation energy and result in diode quality factors higher than one at room temperature [35, 36].

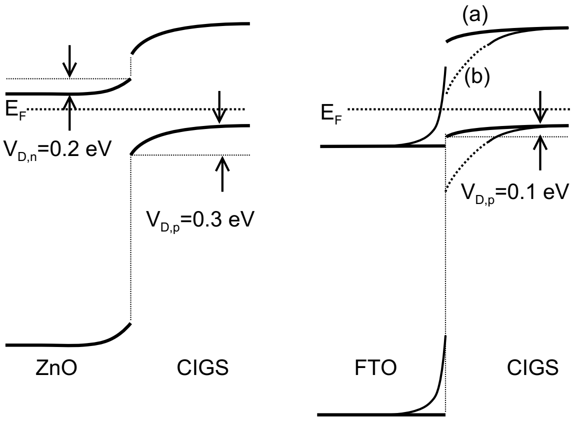

Fig. 4: Band diagram after contact. CIGS/ZnO (left) is in reasonable agreement with the estimated band bending. On CIGS/FTO a band bending of 0.1 eV was measured (a). Based on figure 1 a stronger band bending would be expected (b).

The interpretation of the temperature dependence of the junction between CIGS and FTO is more problematic. The saturation current densities in figure 3 are almost two orders of magnitude higher than in the CIGS/ZnO case, and the fitting of the $j - V$ characteristics is much more difficult. The activation energy of the saturation current is 0.3 eV, resulting in a low $V_{D,p}$ of 0.1 eV. Then, the total band bending is only 0.12 eV.

This behaviour is in contradiction with the proposed band bending and the conduction band offset in figure 1. A low value of the band bending in the absorber could be related to pinning of the Fermi level due to a high density of interface states. For example, pinning positions at $E_g/3$ above the valence band have been reported for a variety of semiconductors in Schottky junctions, resulting in a considerable reduction of the measured barrier heights [37]. Figure 4 illustrates the difficulties of combining the band alignment with the results of the temperature dependent measurements.

The current voltage characteristics of the junction between CIGS and ITO revealed very poor rectifying behaviour and much higher reverse currents, and it was not possible to fit the data reliably.

5. SEMI-TRANSPARENT SOLAR CELLS

The preceeding section showed that the junctions between CIGS and ITO or FTO are unsuitable for superstrate type solar cells. However, the poor rectifying behaviour, particularly of ITO, allows their use as quasi-ohmic contact to CIGS. Semi-transparent substrate solar cells are developed on CIGS/ITO by applying a CdS buffer layer and a ZnO:Al/ZnO front contact. The current voltage characteristics of a semi-transparent solar cell are shown in figure 5. The efficiencies are 6.8%, and 1.5% for illumination through the ZnO front contact (forward) and the ITO back contact (reverse), respectively. A reference solar cell on Mo/glass from the same deposition had an efficiency of 9.7%. A comparison of the characteristics shows lower values in open circuit voltage, short circuit current density, and Fill Factor. A possible explanation for the lower open circuit voltage is the inhibited supply of Na through the ITO [15]. Below the open cicuit voltage the influence of the ITO back contact on series resistance and the corresponding reduction of the Fill Factor is illustrated in figure 5.

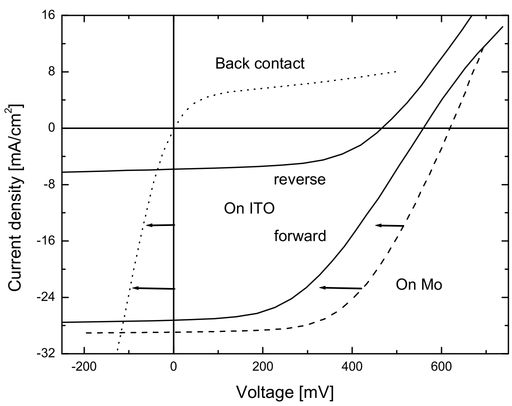

Fig. 5: Current voltage characteristics of the semi-transparent solar cell (full lines) under forward and reverse illumination. Included are the characteristics of the reference solar cell on molybdenum (dashed line) and the the characterisitic of the ITO back contact (dotted line) in order to illustrate the origin of the higher series resistance of the semi-transparent cell (arrows).

Figure 6 compares the quantum efficiencies of the transparent cell measured by illuminating through the ZnO:Al/ZnO/CdS front contact and through the ITO back contact. In the second case it is observed that charge carriers created by short wavelength photons close to the CIGS/ITO interface are lost due to the short diffusion length in the absorber layer.

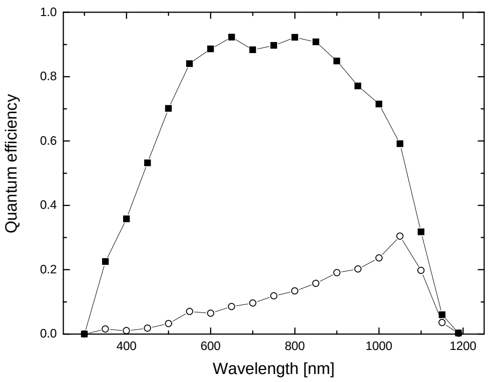

Fig. 6: External quantum efficiencies of the semi-transparent cell. Forward illumination is through ZnO/CdS (full squares), reverse is through the glass/ITO back contact (open circles).

6. CONCLUSIONS

We have investigated the current transport in the heterojunctions of CIGS with ZnO, FTO, and ITO, respectively. The temperature dependence of diode quality factor and saturation current density suggest interface recombination as dominating transport process in CIGS/ZnO. A band bending of about 0.5 eV has been determined, and only about two thirds of it occurs in the CIGS layer. The junction of CIGS to FTO reveals little response to illumination and shows a reduced barrier height, possibly due to a pinning of the Fermi level. The junction of CIGS to ITO shows very poor rectifying behaviour, with its late onset of blocking in reverse direcion it behaves rather ohmic than diode-like, and it has been successfully used as replacement of the metallic back contact for the preparation of semi-transparent CIGS solar cells.

ACKNOWLEDGEMENTS

The financial support of the Gebert Rüf foundation under project GRS-067/00 is thankfully acknowledged.

REFERENCES

[1] M. A. Contreras, B. Egaas, K. Ramanathan, J. Hiltner, A. Swartslander, F. Hasoon, and R. Noufi. Progress toward 20% efficiency in $Cu(In,Ga)Se_2$ polycrystalline thin film solar cells. *Progress in Photovoltaics: Research and Applications*, 7:311–316, 1999.

[2] T. Nakada, K. Matsumoto, and M. Okumura. Improved efficiency of $Cu(In,Ga)Se_2$ thin film solar cells by sulfurization using wet process. In *Proceedings 29th IEEE Photovoltaics Specialists Conference, New Orleans*. IEEE, 2002.

[3] F.-J. Haug, H. Zogg, and A. N. Tiwari. 11% efficiency on CIGS superstrate solar cells without sodium precursor. In *Proceedings 29th IEEE Photovoltaics Specialists Conference, New Orleans*. IEEE, 2002.

[4] T. Nakada and T. Mise. High-efficiency superstrate type CIGS thin film solar cells with graded bandgap absorber layers. In *Proceedings 17th European Photovoltaic Solar Energy Conference, Munich*, volume 2, pages 1027–1030. WIP Renewable Energies, 2001.

[5] D. L. Young, J. Abushama, R. Noufi, X. Li, J. Keane, T. A. Gessert, J. Scott Ward, M. Contreras, M. Smyko-Davies, and T. J. Coutts. A new thin film $CuGaSe_2/Cu(In,Ga)Se_2$ bifacial, tandem solar cell with both junctions formed simultaneously. In *Proceedings of the 29th IEEE Photovoltaics Specialists Conference, New Orleans*, 2002.

[6] T. Nakada, Y. Hirabayashi, and T. Tokado. $Cu(In_{1-x}Ga_x)Se_2$ based thin film solar cells using transparent conducting back contacts. *Japanese Journal of Applied Physics - Letters*, 41(11A):L1209–1211, 2002.

[7] S. Nishiwaki, S. Siebentritt, P. Walk, and M.Ch. Lux-Steiner. A stacked chalcopyrite thin-film tandem solar cell with 1.2 V open circuit voltage. *Progress in Photovoltaics: Research and Applications*, 2003. in press.

[8] A. D. Katnani and G. Margaritondo. Microscopic study of semiconductor heterojunctions: Photemission measurement of the valence-band discontinuity and of the potential barriers. *Physical Review B*, 28(4):1944–1956, 1983.

[9] A. Niemegeers, M. Burgelman, and A. De Vos. On the $CdS/CuInSe_2$ conduction band discontinuity. *Applied Physics Letters*, 67(7):843–845, 1995.

[10] C. Goradia and M. Ghalla-Goradia. Theory of high efficiency $(Cd,Zn)S/CuInSe_2$ thin film solar cells. *Solar Cells*, 16:611–630, 1986.

[11] T. Minemoto, Y. Hashimoto, T. Satoh, T. Negami, H. Takakura, and Y. Hamakawa. $Cu(In,Ga)Se_2$ solar cells with controlled conduction band offset of window/$Cu(In,Ga)Se_2$ layers. *Journal of Applied Physics*, 89(12):8327–8330, 2001.

[12] T. Minemoto, T. Matsui, H. Takaura, Y. Hamakawa, T. Negami, Y. Hashimoto, T. Uenoyama, and M. Kitagawa. Theoretical analysis of the effect of conduction band offset of window/CIS layers on performance of CIS solar cells using device simulation. *Solar Energy Materials and Solar Cells*, 67:83–88, 2001.

[13] V. Nadenau, D. Braunger, D. Hariskos, M. Kaiser, Ch. Köble, A. Oberacker, M. Ruckh, U. Rühle, R. Schäffler, D. Schmid, T. Walter, S. Zweigart, and H.-W. Schock. Solar cells based on $CuInSe_2$ and related compounds: Material

and device properties and processing. *Progress in Photovoltaics: Research and Applications*, 3:363–382, 1995.

[14] J. Sterner, C. Platzer-Björkman, and L. Stolt. XPS/UPS monitoring of ALCVD ZnO growth on $Cu(In,Ga)Se_2$ absorbers. In *Proceedings 17th Euopean Photovoltaic Solar Energy Conference, Munich*, volume 2, pages 1118–1121. WIP Renewable Energies, 2001.

[15] F.-J. Haug, D. Rudmann, G. Bilger, H. Zogg, and A. N. Tiwari. Comparison of structural and electrical properties of $Cu(In,Ga)Se_2$ for superstrate and substrate solar cells. *Thin Solid Films*, 403-404:293–296, 2002.

[16] D. Niles, D. Rioux, and H. Höchst. A photoemission investigation of the SnO_2/CdS interface: A front interface study of CdS/CdTe solar cells. *Journal of Applied Physics*, 73(9):4586–4590, 1993.

[17] D. Schmid, M. Ruckh, F. Grunwald, and H.-W. Schock. Chalcopyrite/defect chalcopyrite heterojunctions on the basis of $CuInSe_2$. *Journal of Applied Physics*, 73(6):2902–2909, 1993.

[18] A. E. Rakhshani, Y. Makdisi, and H. A. Ramazniyan. electronic and optical properties of fluorine-doped tin oxide films. *Journal of Applied Physics*, 83(2):1049–1057, 1998.

[19] E. Burstein. Anomalous optical absorption in InSb. *Physical Review*, 93(3):632–633, 1954.

[20] A. P. Roth, J. B. Webb, and D. F. Williams. Band gap narrowing in heavily defect doped ZnO. *Physical Review B*, 25(12):7836–7839, 1982.

[21] A. Klein, J. Fritsche, W. Jaegermann, J. H. Schön, Ch. Kloc, and E. Bucher. Fermi level-dependent defect formation at $Cu(In,Ga)Se_2$ interfaces. *Applied Surface Science*, 166(1-4):508–512, 2000.

[22] M. Rusu, S. Sadewasser, Th. Glatzel, P. Gashin, A. Simashkevich, and A. Jäger-Waldau. Contribution of the ZnSe/$CuGaSe_2$ heterojunction in photovoltaic performances of chalcopyrite-based solar cells. *Thin Solid Films*, 403-404:344–348, 2002.

[23] A. Andersson, N. Johansson, P. Bröms, N. Yu, D. Lupo, and W. R. Salaneck. Fluorine tin oxide als an alternative to indium tin oxide in polymer LEDs. *Advanced Materials*, 10(11):859–863, 1998.

[24] T. Minami. New n-type transparent conducting oxides. *MRS Bulletin*, 25(8):38–43, 2000.

[25] A. Klein. TCO interfaces in thin film solar cells. In *Proceedings 14th Workshop on Quantum Solar Energy Conversion, Salzburg.* http://www.esqsec.unibe.ch/pub129.pdf, 2002.

[26] A. Klein. Electronic properties of In_2O_3 surfaces. *Applied Physics Letters*, 77(13):2009–2011, 2000.

[27] J. Kessler, J. Scholdstrom, and L. Stolt. Rapid $Cu(In,Ga)Se_2$ growth using end point detection. In *Proceedings 28th IEEE Photovoltaic Specialists Conference, Anchorage*, pages 509–512. IEEE, 2000.

[28] F.-J. Haug, Zs. Geller, H. Zogg, and A. N. Tiwari. Influence of deposition conditions on the thermal stability of ZnO:Al films grown by rf magnetron sputtering. *Journal of Vacuum Science and Technology A*, 19(1):171–174, 2001.

[29] U. Rau, A. Jasenek, H.-W. Schock, F. Engelhardt, and Th. Meyer. Electronic loss mechanisms in chalcopyrite based heterojunction solar cells. *Thin Solid Films*, 361-362:298–302, 2000.

[30] U. Rau and H.-W. Schock. Electronic properties of $Cu(In,Ga)Se_2$ heterojunction solar cells - recent achievements, current understanding, and future challenges. *Applied Physics A*, 69:131–147, 1999.

[31] A. Rothwarf. A p-i-n heterojunction model for the thin-film $CuInSe_2$/CdS solar cell. *IEEE Transactions on Electron Devices*, ED-29(10):1513–1515, 1982.

[32] W. A. Miller and L. C. Olsen. Current transport in Boeing (Cd,Zn)/$CuInSe_2$ solar cells. *IEEE Transactions on Electron Devices*, 31(5):654–661, 1984.

[33] F.-J. Haug, M. Krejci, H. Zogg, A. N. Tiwari, M. Kirsch, and S. Siebentritt. Characterization of $CuGaSe_2$/ZnO for superstrate solar cells. *Thin Solid Films*, 361-362:239–242, 2000.

[34] M. Terheggen, H. Heinrich, G. Kostorz, F.-J. Haug, H. Zogg, and A. N. Tiwari. Diffusion of Ga in $Cu(In,Ga)Se_2$/ZnO superstrate solar cells and its impact on the photovoltaic properties. *Thin Solid Films*, 403-404:212–215, 2002.

[35] H. C. Card and E. H. Rhoderick. Studies of tunnel MOS diodes I. Interface effects in silicon Schottky diodes. *Journal of Physics D: Applied Physics*, 4:1589–1601, 1971.

[36] J. Werner, K. Ploog, and H. J. Queisser. Interface state measurements at Schottky contacts: A new admittance technique. *Physical Review Letters*, 57(8):1080–1083, 1986.

[37] D. K. Schroeder and D. Meier. Solar cell contact resitance - A review. *IEEE Transactions on Electron Devices*, ED. 31(5):637–647, 1984.